Chapter 4

Role of thermal noise for the growth kinetics of active model B (Critical mixture

Abbreviations/Acronyms: **ABPs** (active Brownian particles), **AMB** (active model B), **AMBN**(active model B with noise), **CH** (Cahn-Hilliard), **KPZ** (Kardar-Parisi-Zhang), **LS** (Lifshitz and Slyozov), **MIPS** (motility induced phase separation), **PMB** (passive model B), **TRS** (Time reversal symmetry).

4.1 Introduction

In the previous chapters, 2 and 3, we have discussed the phase separation in mixture of active and passive Brownian particles and also in collection of active Brownian particles in presence of disorder in the system using overdamped Langevin equation through microscopic simulation. In the present chapter, we perform the comprehensive study on the role of noise on the ordering kinetics of the collection of active Brownian particles modeled using coarse-grained conserved active model B (AMB). The ordering kinetics of

the system is studied for the critical mixture when quenched from high to low temperature. From the recent studyKoumakis et al. (2013); Pattanayak et al. (2019b), it is seen that ABP shows a directed transport and there is nontrivial dependence of transport speed on the local particle density. When such ABPs are placed in collection, system undergoes a phase separation, at low packing fractions. This phase separation is called as motility induced phase separation (MIPS) and has been studied in various simulations and experiments Cates et al. (2010); Fily & Marchetti (2012); Popescu et al. (2018); Stenhammar et al. (2013); Thompson et al. (2011); Volpe et al. (2011); Wysocki et al. (2014), discussed in details in chapter 3. The phase separation kinetics in corresponding equilibrium or passive colloidal systems is well studied in theory is described by dynamical ϕ^4 - field theories, where ϕ is conserved scalar order parameter field. The model is named as model B (PMB) Hohenberg & Halperin (1977). The theory uses the simplest form of Cahn-Hiliard (CH) equation and gives the time dependence of domain growth as power law $L \sim t^{1/z}$, where z is the growth exponent that comes 3 for this case Cahn & Hilliard (1959); Hohenberg & Halperin (1977). Recent studies Pattanayak et al. (2021a,b); R.Wittkowski & Cates (2014) are done on AMB by introducing an additional term of activity of strength λ in the order parameter update equation of Cahn-Hilliard (CH) equation, which can not be derived from an equilibrium free energy functional. It is found that the activity slows the growth kinetics in active model Redner et al. (2013a) and the asymptotic growth law shows a crossover from early time LS Lifshitz & Slyozov (1961) types growth, which gives diffusive dynamics of the domains with growth exponent $z = 3$ to late time $1/4$ growth for the athermal systems. But the real system always have thermal fluctuation present in it. The ordering kinetics of corresponding equilibrium PMB remains unaffected in the presence of thermal noise Bray (1990, 1994, 2002). The role of thermal fluctuation on kinetics of growing domain in active model is very important as noise in general is multiplicative in nature and significant at the order-disorder interface Stenhammar et al. (2013).

In this chapter, we study the effect of thermal fluctuations on the domain growth kinetics and domain morphology in AMB. We consider the system at critical mixture. Unlike the passive counterpart of model B, the noise is important for the growth kinetics of AMB. Using extensive numerical study as well as dynamic scaling hypothesis we find that asymptotic growth law for AMBN is diffusive Lifshitz-Slyozov (LS) type, whereas as it was reported in previous study that the asymptotic growth is slower with $1/4$ growth exponent for athermal AMB system. The kinetics of the growing domains shows a strong time dependent growth law in the presence of thermal noise. For fixed noise and activity the size of the domain grows with a time dependent growth exponent. The growth exponent shows a crossover from early time 0.33 value to intermediate time 0.25 value and it again reaches from 0.25 to 0.33 asymptotically. The two different scaling functions are found for intermediate time and late times.

The chapter is organized as follows. In Sec. 4.2, we introduce the AMB with multiplicative noise and discuss the numerical and parameter details. In Sec. 4.3, we present detailed numerical and analytical results for domain growth in the AMB. In Sec. 4.4, we summarize our main conclusions.

4.2 Model

We consider an assembly of ABPs on a two-dimensional ($d = 2$) substrate and study the dynamics of the system. The ABPs move at a constant self-propulsion speed v_0, and their characteristic rotation frequency is τ^{-1}. The local density of the ABPs is denoted as $n(\mathbf{r},t)$, where $\mathbf{r}$ is the position vector. The corresponding order parameter is $\psi(\mathbf{r},t) = 2n(\mathbf{r},t) - 1$, so that regions with $\psi > 0$ are enriched in particles. In the simulations, we consider the mean value of $n(\mathbf{r},0) = 0.5$, so that average order parameter $\psi_0(\mathbf{r},t) = 0$ (critical composition), with random small-amplitude fluctuations lies between -0.05 and 0.05. This system can be modeled by a coarse-grained partial differential equation for $\psi(\mathbf{r},t)$.

The derivation of the hydrodynamic equation can be found in Ref. Cates & Tailleur (2015b). The resultant model can be expressed as a continuity equation for the conserved order parameter:

$$\begin{aligned}\frac{\partial}{\partial t}\psi(\mathbf{r},t) &= -\nabla\cdot\mathbf{J}(\mathbf{r},t),\\ \mathbf{J}(\mathbf{r},t) &= -\nabla\mu(\mathbf{r},t),\\ \mu(\mathbf{r},t) &= \frac{\partial\mathscr{F}[\psi]}{\partial\psi(\mathbf{r})},\\ \mathscr{F}[\psi] &= \int d^d r\{\psi(\mathbf{r},t)^2 + |\nabla\psi(\mathbf{r},t)^2| + \psi(\mathbf{r},t)^4\}\end{aligned} \tag{4.1}$$

where $\mathbf{J}(\mathbf{r},t)$ is the current. The corresponding chemical potential is R.Wittkowski & Cates (2014)

$$\mu(\mathbf{r},t) = -\psi(\mathbf{r},t) + \psi(\mathbf{r},t)^3 - \nabla^2\psi(\mathbf{r},t) + \lambda|\nabla\psi(\mathbf{r},t)|^2. \tag{4.2}$$

The above equations are formulated in dimensionless units. These are obtained by rescaling space by a persistence length $v_0\tau$, and time by the relaxation time τ. The chemical potential μ in Eq. (4.2) is the sum of bulk (μ_0) and gradient (μ_1) contributions. The bulk part is the same as for Model B, $\mu_0 = -\psi(r,t) + \psi(\mathbf{r},t)^3$, and is derived from the bulk free-energy density of a symmetric Ginzburg-Landau (GL) ψ^4-field-theory Puri (2009). The gradient term can be written as the sum of two terms, $\mu_1 = \mu_1^p + \mu_1^a$. Here, $\mu_1^p = -\nabla^2\psi$ is derivable from the square-gradient term in the GL free-energy density. The term μ_1^a is the *active term* which gives rise non-zero particle current in the steady state, breaks TRS Solon et al. (2015b); Tailleur & Cates (2008) and has strength λ, which is a tunable parameter in our study. This term is not obtainable as the derivative of a free energy, and its origin is similar to the lowest-order nonlinear interfacial diffusion term in the Kardar-Parisi-Zhang or KPZ equation for surface growth Kardar (1986). The nonlinear gradient term arises due to lateral growth, analogous to the Eden growth of a surface described by a height profile. This term captures the phenomena of deposition of the particles locally normal to the interface and also known as ballistic deposition. It is an active term that provides

a positive feedback that slows down particles in the high-density region, resulting in an accumulation of the particles. The activity strength λ depends on the functional form of the density-dependent speed of the ABPs R.Wittkowski & Cates (2014). There by varying λ, we can control the speed of the particles in the system .Therefore, the proposed update equation for $\psi(\vec{r},t)$ in the AMB is R.Wittkowski & Cates (2014)

$$\frac{\partial}{\partial t}\psi(\mathbf{r},t) = \nabla\cdot\left[\nabla(-\psi+\psi^3-\nabla^2\psi+\lambda|\nabla\psi|^2)+\theta(\mathbf{r},t)\right]. \tag{4.3}$$

The second term on the R.H.S. in Eq. 4.3 refers to the noise term with mean zero and correlation as given by $<\theta(\mathbf{r},t)>=0$ and

$$<\theta_i(\mathbf{r}',t')\theta_j(\mathbf{r}'',t'')>=\eta\,\delta_{ij}\delta(\mathbf{r}'-\mathbf{r}'')\delta(t'-t'') \tag{4.4}$$

where $<...>$ denotes an average over the Gaussian noise ensemble. In Stenhammar et al. (2013) authors considered fluctuations in the order parameter update equation in their coarse-grained study for active Brownian particles (ABPs). In our study, we have implemented the multiplicative noise, which is the function of the local order parameter $\psi(\mathbf{r},t)$ and of the form,

$$\eta = \eta_a\sqrt{(1+\psi(\mathbf{r},t))((1-\psi(\mathbf{r},t))/2)^2} \tag{4.5}$$

The η_a is the strength of multiplicative noise and can be varied from *zero* to 1. The multiplicative nature of noise arise from the local density dependence of the motility in active systems Stenhammar et al. (2013). Further the presence of finite current at the order-disorder interface, make the noise relevant for active model. So the role of noise becomes important along the order-disorder interface, where local density varies significantly.

We numerically integrated Eq. (4.3) on a square lattice of size $L\times L$ with periodic boundary

conditions in both the directions. We used an Euler discretization scheme with mesh sizes $\Delta x = 1.0$ and $\Delta t = 0.01$. The space mesh is small enough to resolve coarsening interfaces, and the time mesh is adequate to ensure stability of the numerical scheme. The initial condition for a run consisted of the order parameter field $\psi(\mathbf{r},0)$ having small-amplitude fluctuations about an average value $\psi_0 = \int \psi(\mathbf{r},t)d^2r = 0$. This case corresponds to a *critical* composition with an equal number of occupied and empty sites. All cases with $\psi_0 \neq 0$ are referred to as *off-critical* compositions. Here we only discuss the results of critical composition. The Eq. (4.3) is numerically integrated for different values of noise strength η_a and activity parameter $\lambda \in (0,8)$. For $\lambda = 0$, and for $\eta_a = 0$ the model reduces to the passive model B (PMB) Cahn & Hilliard (1959); Hohenberg & Halperin (1977); Puri (2009) and for $\eta_a = 0$ and $\lambda \neq 0$, the model reduces to the previously studied cases and referred as active model B (AMB) R.Wittkowski & Cates (2014). The present model is with non-zero noise, $\eta_a \neq 0$ and non-zero activity, $\lambda \neq 0$ and we name it as active model B with noise (AMBN). All results presented here are for lattice sizes $L = 512$, and statistical quantities are averaged over 100 independent runs.

4.3 Results

First, we study the domain morphology and kinetic of the growing domains for the critical composition of the AMBN for different strengths of noise and fixed activity strength $\lambda = 1$. Snapshots of the local density $\psi(\mathbf{r},t))$ are shown in Fig. 4.1, where color bar represents the ψ value. Blue (dark) and orange (bright) regions $\psi(\mathbf{r},t)$ are smaller and higher density than the mean density $\psi = 0$, respectively. The three rows in Fig. 4.1 are for three different times $t = 500$, 5000 and 50000 and different columns are for different strengths of noise . For all noise strengths $\eta_a = AMB$, 0.5, 0.8 and 1, starting from the initial random homogeneous mixed state, the domains of ψ rich regions start to grow with time. In the absence of noise we observe the formation of the isolated domains as

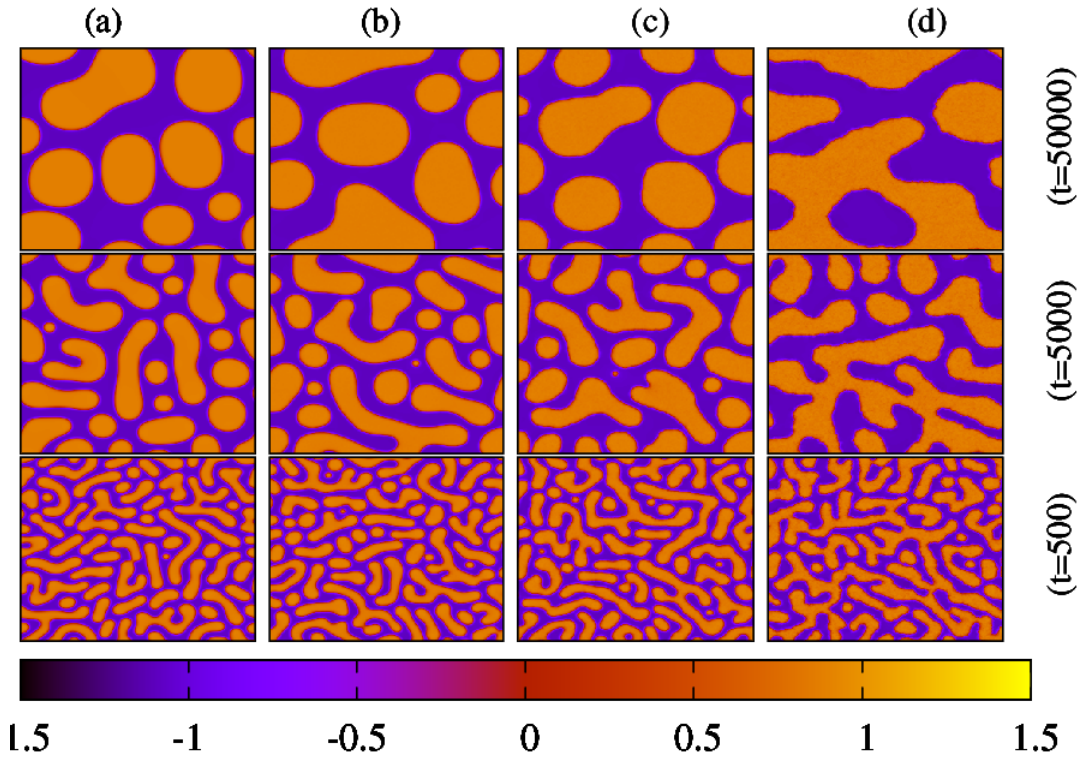

Fig. 4.1 (color online) Time evolution of the system for different values of noise strengths η_a, keeping the activity, λ fixed to 1. (a),(b),(c) and (d) are for noise strengths 0 (AMB), 0.5, 0.8 and 1.0 respectively. The average order parameter value is $\psi_0 = 0$, corresponding to critical composition. The color bar shows the range of ψ value.

shown in Fig. 4.1 (a) (AMB) and also reported in previous study Pattanayak et al. (2021b); R.Wittkowski & Cates (2014). Furthermore, we note that as time progresses the domains become bi-continuous for sufficiently high noise strengths. The snapshot of the local ψ for finite noise strengths is shown in Fig. 4.1(b-d). The domains become bi-continuous for large times and for higher noise strength $\eta_a = 1.0$.

Domain length and growth exponent

To quantify the kinetic of the growing domains of AMBN, we calculate the order parameter two-point correlation function defined as

$$C(r,t) = < \psi(\mathbf{r}_0 + \mathbf{r}, t)\psi(\mathbf{r}_0, t) > \tag{4.6}$$

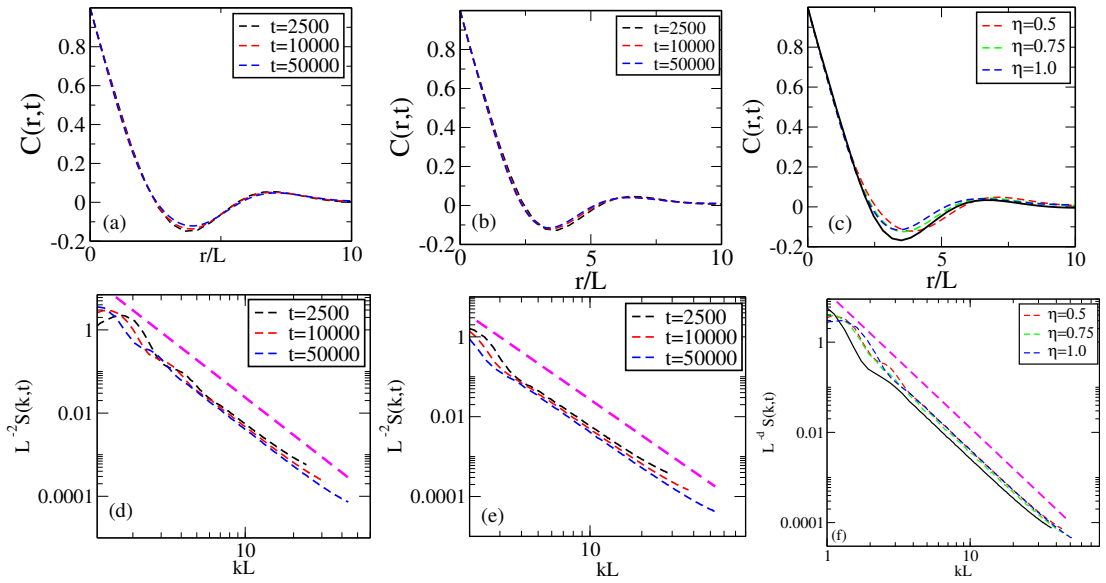

Fig. 4.2 (color online) (a) and (b) show the dynamical scaling of correlation function for two different values of the noise strengths 0.5 and 1.0 respectively and compared them with the passive binary mixture.The dashed lines indicate different time for each noise strength. The value of the activity is 1 for all three cases.(c) shows the static scaling for different noise strengths, 0.5, 0.75 and 1.0 at t=50000. (d) and (e) show the dynamical scaling for structure factor for two different values of the noise strengths 0.5 and 1.0 respectively and compared them with the passive binary mixture. (f) shows the scaled static structure factor for same set of parameters. Black solid line represents the PMB. Magenta dashed line shows the line of slope -3

where the angular brackets $< .. >$ represent the average over reference position $\mathbf{r}_0$, 100 independent realisations followed by spherical averaging. Fig 4.2(a) and (b) respectively shows the scaled correlation function for different noise strengths, $\eta_a = 0.5$ and 1.0 at different times. In fig 4.2(a-b), different colors represent the different times. We observe that for each noise strength, the system shows good dynamic scaling that means the morphology of domains does not change with time and the domain structures are statistically similar apart from a scale factor that is defined as characteristic scale $L(t)$ and is discussed further. Fig 4.2(c) shows the static scaling for fixed time $t = 50000$ and different $\eta_a = 0.5, 0.75$ and 1.0 . For comparison we have also shown the plot for PMB at the same time. We noticed that AMBN curves closer to PMB as we increase the noise strength. We also calculate the structure factor, which is the Fourier transform of real-space

correlation function

$$S(\vec{k},t) = \int d\vec{r} e^{i\vec{k}\vec{r}} C(\vec{r},t) \tag{4.7}$$

The lower panel plots of fig. 4.2 shows the scaled structure factor $L^{-d}S(k,t)$ vs. kL for the same set of parameters as for the correlation function in the upper panel. The data collapse is observed onto a scaling function and at late time the tail of the structure factor shows a power law decay $S(k,t) \sim k^{-(d+1)}$, $d = 2$ in our case, which corresponds with the Porod's tail **?**. In fig 4.2(f) we have plotted the data for PMB also, that gives good comparison with AMBN curves.

Next we define the domain size, $L(t)$ as the characteristic scale over which the correlation function, $C(r,t)$ stays to 0.5 of its maximum value at $r = 0$. The evolution morphology of the domain is characterised by this single length scale, $L(t)$. We plot $L(t)$ vs. t in fig. 4.3(a) on log-log scale for $\eta_a = 0.5$, 0.75, 0.85 and 1.0 keeping the value of activity λ fixed to 1.0. Domain length for PMB and AMB is also included here. It is found that Puri (2009) Pattanayak et al. (2021a,b); R.Wittkowski & Cates (2014) ordering kinetics of domain growth for AMB shows a growth law scales as $L(t) \sim t^{1/z}$, where z is the dynamic growth exponent. For PMB Puri (2009), $z = 3$ and for AMB, z shows a crossover from 3 to 4. The asymptotic growth is $z = 4$ for AMB Pattanayak et al. (2021a,b). In our present study with non-zero thermal noise, we found that the asymptotic growth for all noise strength is again similar to as reported for PMB and $z = 3$. Although for intermediate time it deviates from $z = 3$. Further, to characterise the time dependence of domain length we calculate the effective growth exponent, $\frac{1}{z_{eff}}$ as a function of time t, which is defined as

$$\frac{1}{z_{eff}} = \frac{d(lnL(t))}{d(lnt)} \tag{4.8}$$

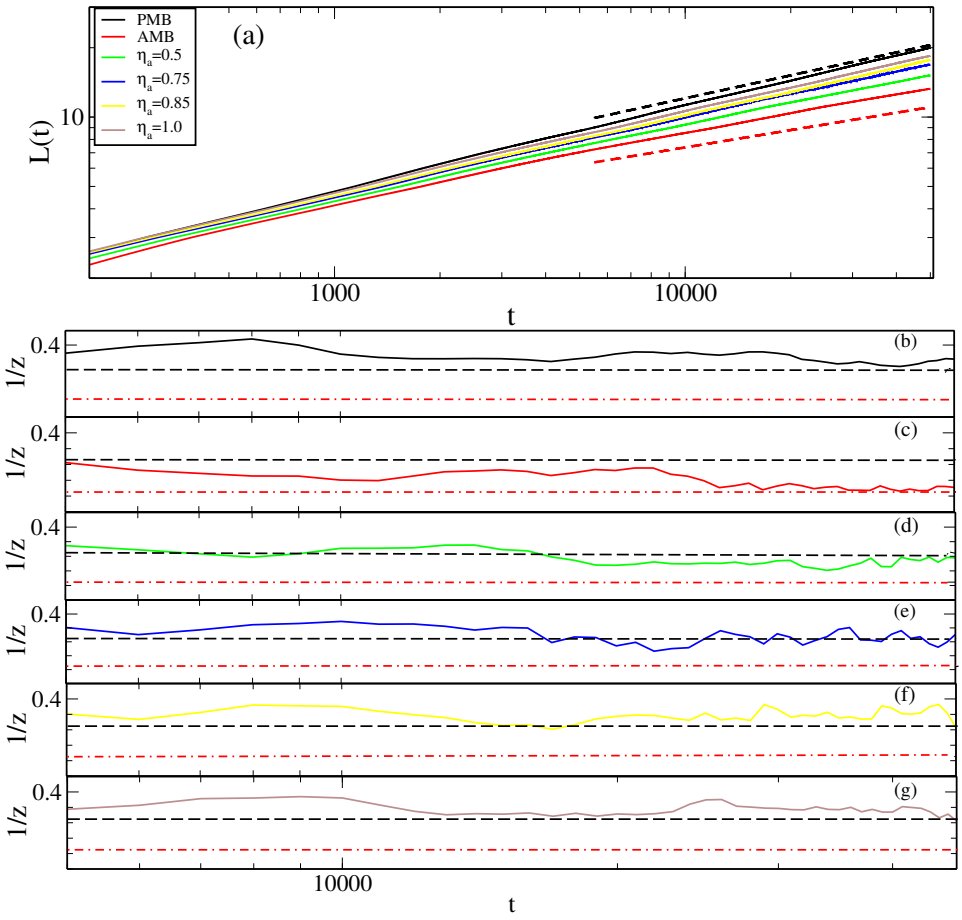

Fig. 4.3 (color online) Log-Log plot of $L(t)$ vs. t is shown in (a) for different noise strengths, η_a and compared with PMB and AMB. Black and red dashed lines are the lines of slope $1/3$ and $1/4$ that show the power law of growth as $L(t) \sim t^{1/3}$ and $L(t) \sim t^{1/4}$ respectively. $(b)-(g)$ shows the effective exponent $1/z$ vs. t for same set of parameters as in (a). In each frame, $(b)-(g)$, the horizontal black and red dashed lines are drawn at $1/z = 1/3$ and $1/z = 1/4$ respectively.

In fig 6.4(b-g), we plot $\frac{1}{z_{eff}}$ for the same set of parameters as in Fig 4.3(a). For PMB 4.3(b) and AMB 4.3(c), the $\frac{1}{z_{eff}}$ clearly goes to 0.33 and 0.25 respectively at late times. For finite noise and for all noise strengths Fig 4.3(d-g) and for $\lambda = 1.0$ the $\frac{1}{z_{eff}}$ approaches to 0.33 at late times.

Till now, we have found that the value of $\frac{1}{z_{eff}}$, which is 0.33 at late time for all strengths of noise for fixed activity $\lambda = 1$. We further look at the morphology and structure of

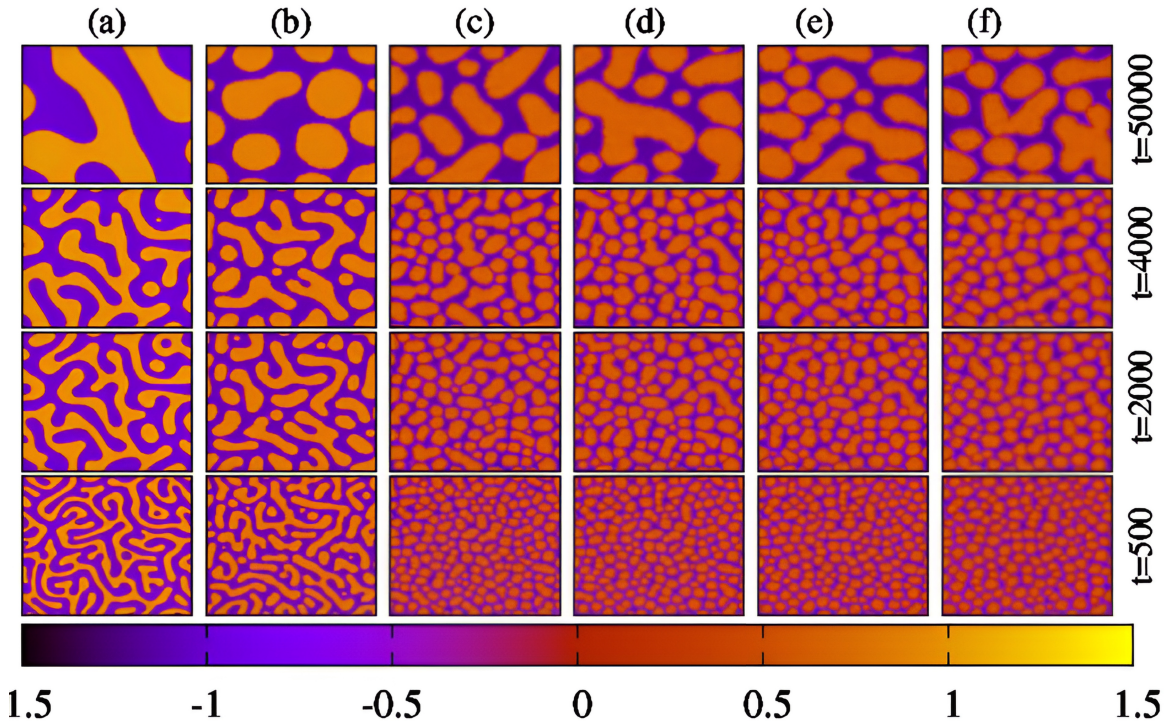

Fig. 4.4 (color online) Time evolution of the system is shown for different activities left to right panel and for fixed moderate strength of noise $\eta_a = 0.5$. $(a)-(f)$ are for activities $\lambda = 0$ (PMB), 1, 4, 5, 6 and 8 respectively. The average order parameter value is $\psi_0 = 0$, corresponding to critical composition. The color bar shows the range of ψ value.

domains for large activity and moderate noise strength $\eta_a = 0.5$. In Fig. 4.4(a-f) we show the real time snapshots of local ψ for four different times $t = 500$, 2000, 4000 and 50000, for fixed noise strength $\eta_a = 0.5$ and different activities of AMBN varied from 1, 4, 5, 6 and 8 and for the comparison we have also included the snapshots for PMB for the same times. For PMB, the structure of domain is bi-continuous or connected domains are found for all times. For lower activity $\lambda = 1.0$, the structure of the domains remains bi-continuous for all time with small deviation at later times, whereas as we go for higher activities $\lambda \geq 4$, the early time domains are isolated and they get elongated at late times. To further quantify the effect of such structure on the kinetics of domain we calculate the $1/z_{eff}$ for the same set of parameters $(\lambda, \eta_a) = ([1-8], [0.5])$. In fig. 4.5(a-e) we show the time dependence of $1/z_{eff}$ for different $\lambda = 1$, 4, 5, 6 and 8 respectively. It is

found that for $\lambda = 6$ and 8, for early time $1/z_{eff}$ shows a quick approach to 0.25 and then shows a small plateau for intermediate time and then again shows a slow crossover to 0.33 at late time times. As we decrease λ, the $1/z_{eff}$ still shows the early time dip to lower values and before it reaches to 0.25, it starts increasing and asymptotically approaches to 0.33. For small $\lambda = 1$, the dip is small such that $1/z_{eff}$ cannot reach to 0.25 and we always find the late time 0.33 behaviour. Now we can say that for large $\lambda > 4$, the effective exponent $1/z_{eff}$ shows the three different regime. For early time when activity dominates, it shows a crossover from 0.33 to 0.25 as reported in previous study of AMB Pattanayak et al. (2021b), then for intermediate times, the exponent remains to the lower values and then at late time noise dominates and we find the exponent 0.33. The same is observed in the real space snapshots, where for larger $\lambda > 4$, early time domains are isolated and becomes elongated for late times. The first crossing time from 0.33 to 0.25, depends on the magnitude of λ and decreases by increasing λ algebraically $\lambda^{-3/2}$ as reported for AMB Pattanayak et al. (2021b). Since for lower λ the crossing time is large, hence before the activity dominates, noise takes over and the growth exponent is always 0.33 and structure of the domain is elongated as shown in Fig. 4.1.

Now we further calculate the two-point density correlation function for the early, intermediate and late times and for fixed activity $\lambda = 8$ and nosie strength $\eta_a = 0.5$. As shown in Fig.4.5 (f) and (g) we plot the scaled two-point correlation function and structure factor respectively. Different plots are for different times. The first two times are selected as $t = 200$ and 400, specified as early time, when the growth law descends from 0.33 to 0.25 value, then we select the intermediate time when activity dominates and the growth law is 0.25 and finally the late time or asymptotic limit when noise stand over and growth law is 0.33. We clearly find the good scaling collapse of data for intermediate and late times and for late time scaled correlation comes closer to the correlation for PMB as shown by black solid line. Hence with respect to time two-different scaling functions are found for

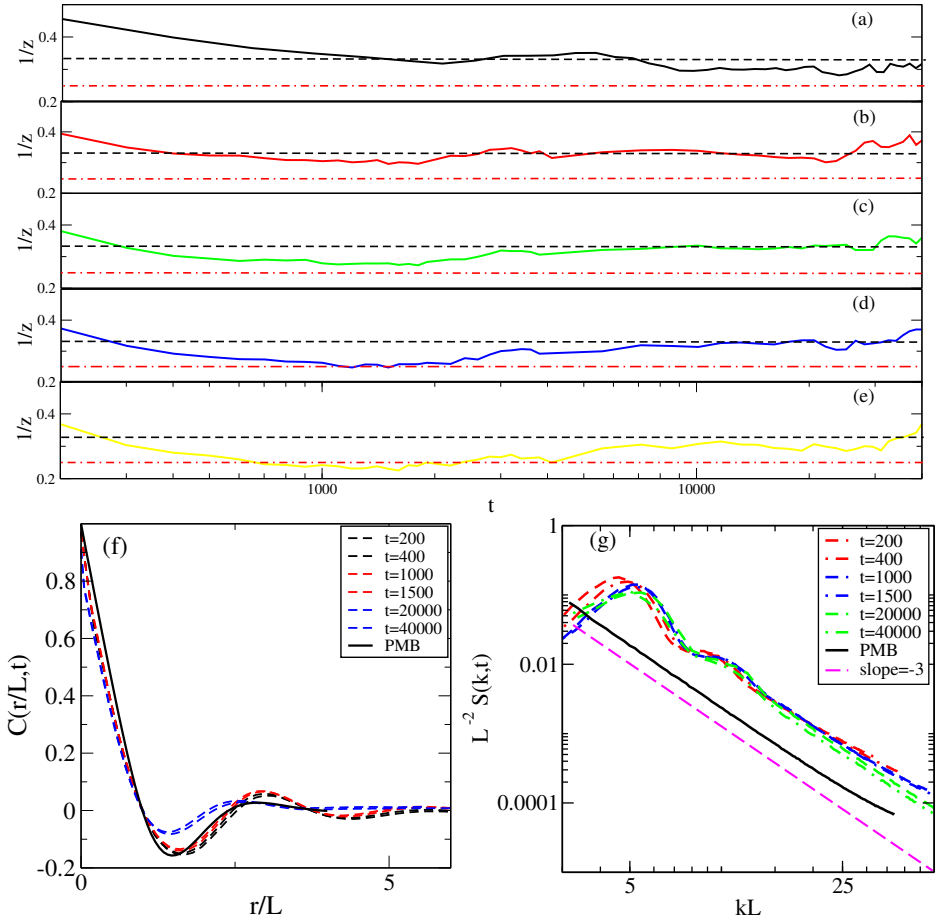

Fig. 4.5 (color online) $(a)-(e)$ show the effective exponent for activity $\lambda = 1,4,5,6$ and 8 for fixed strength of noise 0.5. Black and red horizontal dashed lines are drawn at $1/3$ and $1/4$ respectively. Scaled Correlation function and structure factor are shown in (f) and g is for activity 8. Strength of noise is fixed to 0.5. All plots are shown for three different time regimes, starting from very early time. Black solid line is for PMB. Magenta dashed line is line of slope -3.

intermediate and late times. The right panel plot of Fig. 4.5(g) shows the scaled structure factor for the same range of time and similar conclusion can be made from structure factor. Also the morphology of the domains follows the Porod's tail Porod (1951) and tail of the structure factor decay as $(kL)^{-3}$.

In the next section we focus our attention to scaling theory of PMB and AMBN. We will first show that thermal noise is irrelevant for PMB whereas it is relevant for the AMBN.

4.3.1 Scaling Theory

Scaling for PMB:- We start with the Langevin equation for a conserved density field

$$\frac{\partial \psi(r)}{\partial t} = \alpha \nabla^2 \frac{\delta \mathscr{F}}{\delta \psi(r)} + \eta(r,t) \tag{4.9}$$

$\mathscr{F}\{\psi(\mathbf{r},t)\}$ is the free-energy functional and α is the mobility factor set to 1 in Eq. 4.9. $\eta(r,t)$ is a Gaussian white noise generated by thermal fluctuations with mean zero and correlations $\eta(r,t)\eta(r',t') = 2\alpha T \nabla^2 \delta(r-r')\delta(t-t')$. Introducing the Fourier component $\psi_k(t) = V^{-1/2}\int d^d r \psi(r,t)\exp(i\mathbf{k}.\mathbf{r})$, V is area of the space, the equation in Fourier space we get

$$\frac{\partial \psi_k}{\partial t} = -k^2 \alpha \frac{\partial \mathscr{F}}{\partial \psi_{-k}} + \eta_k \tag{4.10}$$

$$\frac{1}{\alpha k^2}\frac{\partial \psi_k}{\delta t} = -\frac{\partial \mathscr{F}}{\partial \psi_{-k}} + \xi_k(t) \tag{4.11}$$

where $\xi_k(t) = \frac{\eta_k}{\alpha k^2}$ Introducing rescaling of space and time, $k = k'/b$ and $t = b^z t'$ leads $\psi_k(t) = \psi_{k'/b}(b^z t') = b^\zeta \psi'_{k'}(t')$ and $\mathscr{F}(\psi_k) = b^y \mathscr{F}(\psi'_{k'})$ which gives

$$\frac{b^{2-z+\zeta}}{\alpha k'^2}\frac{\partial \psi'_{k'}}{\partial t'} = -b^{y-\zeta}\frac{\partial \mathscr{F}'}{\partial \psi'_{-k'}} + \xi_{k'/b}(b^z t') \tag{4.12}$$

$$\frac{b^{2-z-y+2\zeta}}{\alpha k'^2}\frac{\partial \psi'_{k'}}{\partial t'} = -\frac{\partial \mathscr{F}'}{\partial \psi'_{-k'}} + b^{-y+\zeta}\xi_{k'/b}(b^z t') \tag{4.13}$$

$$\frac{b^{2-z-y+2\zeta}}{\alpha k'^2}\frac{\partial \psi'_{k'}}{\partial t'} = -\frac{\partial \mathscr{F}'}{\partial \psi'_{-k'}} + \xi'_{k'}(b^z t') \tag{4.14}$$

where the new noise $\xi'_k(t)$ is $< \xi'_{k'}(t'_1)\xi'_{-k'}(t'_2) >= b^2 b^{-z} b^{-2y+2\zeta}\frac{2T}{\alpha k'^2}\delta(t'_1 - t'_2)$

$$< \xi'_{k'}(t_1)\xi'_{-k'}(t_2) >= b^{2-z+2\zeta-2y}\frac{2T}{\alpha k'^2}\delta(t'_1 - t'_2) \tag{4.15}$$

$$\frac{1}{\alpha' k'^2}\frac{\partial \psi'_{k'}}{\partial t'} = -\frac{\partial \mathscr{F}'}{\partial \psi_{-k'}} + \xi'_{k'}(t') \tag{4.16}$$

where $< \xi'_{k'}(t'_1)\xi'_{-k'}(t'_2) >= \frac{2T'}{\alpha k'^2}\delta(t'_1 - t'_2)$ and $(\frac{1}{\alpha})' = (\frac{1}{\alpha})b^{2-z-y+2\zeta}$ (from eq 4.13)

Putting the value of $1/\alpha$ in equation 4.15 we have

$$< \xi'_{k'}(t_1)\xi'_{-k'}(t_2) >= \frac{2Tb^{2-z+2\zeta-2y}}{\alpha' b^{2-z-y+2\zeta}k'^2}\delta(t_1 - t_2) \tag{4.17}$$

this yields

$$< \xi'_{k'}(t_1)\xi'_{-k'}(t_2) >= \frac{2Tb^{-y}}{\lambda' k'^2}\delta(t_1 - t_2) \tag{4.18}$$

$$T' = Tb^{-y} \tag{4.19}$$

where, $b > 1$ and $y > 0$, so $T' \to 0$ and we find temperature is irrelevant. And for the growth exponent we have

Now, coming for the growth exponent,

$(\frac{1}{\alpha})' = (\frac{1}{\alpha})b^{2-z-y+2\zeta}$ from equlibrium theory, $y = d-1$ and $\zeta = \frac{d}{2}$ this leads to

$$\frac{1}{\alpha}' = \frac{1}{\alpha}b^{3-z} \tag{4.20}$$

Since, $z > 3$ and $z < 3$ is not possible because it will make the Hamiltonian irrelevant. So imposing the condition of self similarity will lead to $z = 3$, giving the result for PMB.

Scaling for AMBN:- We start with rescaling of space and time as before $k = \frac{k'}{b}$, $t = b^z t'$, $\psi_k(t) = b^\zeta \psi_{k'}(t')$ and $\mathscr{F}(\psi_k) = b^y \mathscr{F}'(\psi'_{k'})$. The multiplicative noise in AMBN is as given in Eq. 4.5 $\eta = \eta_a\sqrt{(1+\psi)(1-\psi)^2} \backsimeq \eta_a \psi^{3/2}$. Hence for AMBN

$$\frac{\partial \psi}{\partial t} = \alpha\nabla^2\frac{\delta \mathscr{F}}{\delta \psi} + \lambda\nabla^2(\nabla\psi)^2 + \nabla.\eta \tag{4.21}$$

writing in Fourier space

$$\frac{\partial \psi_k}{\partial t} = -\frac{\alpha k^2 \mathscr{F}}{\partial \psi_{-k}} + \lambda k^4 \psi_k \psi_{-k} + \xi_k \tag{4.22}$$

and rescaling of space, time and fields in dimensionless units

$$\frac{b^{2-z+\zeta}}{\alpha k'^2}\frac{\partial \psi_{k'}}{\partial t'} = -b^{y-\zeta}\frac{\partial H'}{\partial \psi' - k'} + \frac{\lambda}{\alpha} b^{-2} k'^2 b^{2\zeta} \psi_{k'}(t')\psi_{-k'}(t') + \xi' \tag{4.23}$$

$$\begin{aligned} \frac{b^{2-z-y+2\zeta}}{\alpha k'^2}\frac{\partial \psi_{k'}}{\partial t'} &= -\frac{\partial \mathscr{F}'}{\partial \psi' - k'} \\ + \frac{\lambda}{\alpha} b^{-2+3\zeta-y} k'^2 \psi_{k'}(t')\psi_{-k'}(t') &+ \xi' \end{aligned} \tag{4.24}$$

where

$$< \xi'(t_1')\xi'(t_2') > = b^{-2y+2\zeta}\frac{2Tb^2}{\alpha k'^2} b^{3\zeta-z}\delta(t_1' - t_2') \tag{4.25}$$

this gives

$$< \xi'\xi' > = b^{-2y+5\zeta+2-z}\frac{2T}{\alpha k'^2}\delta(t_1' - t_2') \tag{4.26}$$

From eq 4.24 , we can obtain; $\frac{1}{\alpha'} = \frac{1}{\alpha} b^{2-z-y+2\zeta}$ hence

$$< \xi(t_1')\xi'(t_2') > = \frac{b^{5\zeta-2y+2-z}}{\alpha' b^{2-z-y+2\zeta}}\frac{2T}{k'^2}\delta(t_1' - t_2') \tag{4.27}$$

gives

$$T' = T b^{3\zeta-y} \tag{4.28}$$

For the condition that if the temperature is irrelevant lead to $3\zeta - y < 0$, which implies $3\zeta < y$ and if we take $\zeta = \frac{d}{2}$ and $y = d-1$ from equilibrium theory Cahn & Hilliard (1959) we get $\frac{3d}{2} < d-1$ and for 2 dimension it implies $3 < 1$. So, we can argue that the temperature is no longer an irrelevant variable for AMBN. Now, checking the growth

exponent leads us the value $z = 3$ as found in our numerical result. we check how λ is going to be change in this case. From second term in equation (22) we get

$$\frac{\lambda b^{-2+3\zeta-y}}{\alpha} = \frac{\lambda'}{\alpha'} \tag{4.29}$$

$$\lambda' = \frac{\lambda \alpha' b^{-2+3\zeta-y}}{\alpha} \tag{4.30}$$

this gives $\lambda' = \frac{\lambda \alpha' b^{-2+3\zeta-y}}{\alpha' b^{2-z-y+2\zeta}}$ or

$$\lambda' = \lambda b^{-4+z+\zeta} \tag{4.31}$$

since $\zeta = \frac{d}{2}$ leads the value of exponent $z = 3$, the same is found in our numerical study asymptotically.

4.4 Discussion

We have executed a detailed numerical study of AMB with noise or AMBN. The noise introduced here is multiplicative in nature and important at the order disorder interface. The ordering kinetics of the system is studied for different strengths of the noise. The results are compared with our recent study of ordering kinetics in AMB Pattanayak et al. (2021b) and passive model B Puri (2009). When quenched from the random disordered state to an ordered state for AMB, the size of the ordered domains increases with time with an effective asymptotic growth exponent 0.25 as found in our previous study Pattanayak et al. (2021b). Unlike the PMB, we find the noise or temperature is a relevant for AMBN. Using extensive numerical study we find that the noise changes the asymptotic effective growth exponent from $1/4$ to $1/3$ in AMBN and structure of the domains changes from spherical isolated domains to bi-continuous elongated domain. For fixed noise and activity the size of the domain grows with a time dependent growth exponent. For early to intermediate times, the growth exponent shows a crossover from early time 0.33 value to intermediate

time 0.25 value and finally at late time it goes to 0.33. Correspondingly the two different scaling functions are found for intermediate time with growth exponent 0.25 and late time with growth exponent 0.33 and late time scaling function slowly converge towards the scaling function of PMB.

Further the role of noise for the system away from the critical composition is also an interesting problem to study which we discuss in the next chapter. Since the noise is intrinsic to real experimental systems. The role of noise in ordering kinetics in active models is an interesting direction to understand the effect of thermal fluctuations in other active systems Chari et al. (2019); Chattopadhyay et al. (2021, 2023); Tjhung et al. (2018); Toner (2012).

****